

Giant and reversible enhancement of the electrical resistance of GaAs_{1-x}N_x by hydrogen irradiation

J. Alvarez and J.-P. Kleider

Laboratoire de Génie Électrique de Paris, CNRS UMR8507, SUPELEC, Univ. Paris-Sud, UPMC Univ. Paris 06; 11 rue Joliot-Curie, Plateau de Moulon, F-91192 Gif-sur-Yvette Cedex, France

R. Trotta, A. Polimeni,* and M. Capizzi

Dipartimento di Fisica, Sapienza Università di Roma, P.le A. Moro 2, 00185 Roma, Italy

F. Martelli and L. Mariucci

IMM-CNR, via del Fosso del Cavaliere 100, 00133 Roma, Italy

S. Rubini

TASC-IOM-CNR, Area Science Park, S.S. 14, Km. 163.5, 34012 Trieste, Italy

(Received 7 June 2011; revised manuscript received 31 July 2011; published 31 August 2011)

The electrical properties of untreated and hydrogen-irradiated GaAs_{1-x}N_x are investigated by conductive-probe atomic force microscopy (CP-AFM). After hydrogen irradiation, the resistance R of GaAs_{1-x}N_x increases by more than three orders of magnitude while that of a N-free GaAs reference slightly decreases. Thermal annealing at 550 °C of H-irradiated GaAs_{1-x}N_x restores the pristine electrical properties of the as-grown sample thus demonstrating that this phenomenon is fully reversible. These effects are attributed to the nitrogen-hydrogen complexes that passivate N in GaAs_{1-x}N_x (thus restoring the energy gap of N-free GaAs) and, moreover, reduce the carrier scattering time by more than one order of magnitude. This opens up a route to the fabrication of planar conductive/resistive/conductive heterostructures with submicrometer spatial resolution, which is also reported here.

DOI: [10.1103/PhysRevB.84.085331](https://doi.org/10.1103/PhysRevB.84.085331)

PACS number(s): 71.55.Eq, 73.61.Ey, 78.55.Cr, 72.80.Ey

I. INTRODUCTION

It has been well documented that hydrogen modifies the electronic, optical, and structural properties of dilute nitrides,¹ e.g., GaAs_{1-x}N_x, In_yGa_{1-y}As_{1-x}N_x, and GaP_{1-x}N_x. In fact the incorporation of atomic hydrogen in GaAs_{1-x}N_x and related materials neutralizes N effects² in the host lattice via the formation of peculiar N- n H complexes, as shown by infra-red³ and x-ray⁴ absorption measurements. Specifically, two hydrogen atoms bind *not* equivalently to a same N atom and form a N-2H complex with C_{1h} symmetry.³ In turn this brings band-gap energy,⁵ electron-effective mass and g-factor,^{6,7} refractive index,⁸ and lattice constant⁴ back to the values of the N-free host (GaAs), while a third H atom causes an overshooting of the lattice constant with respect to that of GaAs.⁴

The patterning of the spatial distribution of these complexes by a masked hydrogenation method⁹ and the extremely steep forefront of H diffusion profile¹⁰ has made it possible to modify in the growth plane the band-gap energy² and strain⁹ with high spatial precision. Very recently, site-controlled GaAs_{1-x}N_x quantum dots have been fabricated by this approach.¹¹ Despite the dramatic changes induced by H on the physical properties of dilute nitrides, the opportunity to modify the *electric and transport* characteristics of these materials has thus far never been explored.

In this work we map the local electrical resistance (R) of hydrogenated GaAs_{1-x}N_x by conductive-probe atomic force microscopy (CP-AFM). Following H incorporation, R increases by more than three orders of magnitude in GaAs_{1-x}N_x samples with different N concentration, while it slightly decreases in N-free GaAs. Thermal annealing of

GaAs_{1-x}N_x:H restores the pristine electrical properties of the as-grown sample thus showing that this phenomenon is fully reversible. These H-induced variations of R follow those observed in the optical/electronic properties (e.g., band-gap energy). The decrease in intrinsic carrier concentration produced by the re-establishment of the N-free GaAs band-gap energy upon hydrogenation accounts only for a part of the observed increase in the local electrical resistance, which calls for a reduction of the carrier scattering time by one order of magnitude. Finally, we demonstrate that an in-plane patterning of the electrical resistance of a GaAs_{1-x}N_x chip is achievable down to a submicrometer scale.

II. EXPERIMENTAL

Different GaAs_{1-x}N_x samples were grown at 500 °C by molecular beam epitaxy on top of a 500-nm-thick GaAs buffer deposited at 600 °C on a (001) semi-insulating GaAs substrate. The GaAs_{1-x}N_x epilayers have thickness $t = 200$ nm ($x = 0.9\%$) and no GaAs cap layer, $t = 280$ nm ($x = 1.27\%$), and $t = 138$ nm ($x = 1.95\%$) with GaAs cap layer equal to 20 nm. A GaAs control sample with the same-layer thickness and growth temperature sequence of the $t = 200$ nm sample was also grown.

Samples were irradiated at 300 °C with different doses, d_H , of low-energy (100 eV) H⁺ ions. A series of 50-nm-thick Ti wires, opaque to hydrogen, were deposited by electron-beam lithography on the $x = 0.9\%$ sample (wire width $w = 5, 2, 1$, and $0.5 \mu\text{m}$, separated from each other by $20 \mu\text{m}$) in order to impede H diffusion in defined regions of the sample.^{2,9} Before characterization, the Ti wires were removed by HF. Annealing

experiments were performed at 550°C under high vacuum (8×10^{-7} mbar) in order to dissociate N-H complexes.⁷

Local resistance measurements were performed by CP-AFM¹² in patterned and unpatterned specimens, all hydrogenated under similar conditions. The experimental set-up for resistance measurements was based on a Digital Instruments Nanoscope IIIa Multimode atomic force microscope associated with a home-made extension “Resiscope”¹³ designed to apply a stable DC bias voltage (± 0.01 –10 V) to the sample. The resulting current through the tip was measured while the sample surface was scanned in contact mode. Local resistance values in the range 10^2 – 10^{12} Ω can be measured with a few percent accuracy for a ± 1 V bias voltage. Conducting probes made of silicon coated by boron-doped polycrystalline diamond, with an intermediate spring constant of about 2 N/m, were suitable for our experimental conditions, where measured R values are much greater than the probe intrinsic resistance ($\sim 10^4$ Ω). The scanned area is typically (1×1) μm^2 and made of 512×512 pixels. We point out that the overall resistance in CP-AFM measurements is commonly controlled by the contact resistance between the AFM probe tip and the sample.¹⁴

The electronic properties of the structures were determined by micro-photoluminescence, μ -PL, (using a 20 \times objective) and macro-PL, both excited by a $\lambda = 532$ nm laser, spectrally analyzed by a 0.75-m-long monochromator and detected by an InGaAs linear array detector.

All measurements were performed at room temperature.

III. RESULTS AND DISCUSSION

Figure 1(a) shows by *larger symbols* the local resistance values measured for the $\text{GaAs}_{1-x}\text{N}_x$ sample with $x = 0.9\%$ after different treatments (smaller symbols refer to a GaAs reference to be discussed later). Hydrogen irradiation ($d_H = 3 \times 10^{18}$ cm^{-2}) determines an *increase* of R by a factor ~ 400 with respect to the untreated sample.¹⁵ At the same time, PL measurements indicate a complete passivation of the electronic activity of N, namely, a blue-shift of the $\text{GaAs}_{1-x}\text{N}_x$ band-gap energy (1.255 eV) to the GaAs value (1.422 eV); see Fig. 1(b). Thermal annealing of the hydrogenated sample for 1 hour at 550°C dissociates nitrogen-hydrogen complexes^{4,5} and brings back the band-gap energy of the untreated $\text{GaAs}_{1-x}\text{N}_x$ sample; see the topmost spectrum in Fig. 1(b). In the same sample R reduces by a factor 1900, primarily because of a removal of H atoms out of the lattice, and reaches a value smaller by a factor of approximately 5 with respect to that measured in the untreated (starting) material. This additional decrease is ascribable to an improvement of the crystal quality caused by the high-temperature treatment. In fact a similar R decrease has been observed in an untreated, H-free $\text{GaAs}_{1-x}\text{N}_x$ sample subjected to a same 1 hour annealing at 550°C.

In order to ascertain the role of N and H-related complexes on the electrical behavior of $\text{GaAs}_{1-x}\text{N}_x$, we studied a GaAs reference sample. Figure 1(a) shows by *smaller symbols* the values of the local resistance of the reference sample before and after hydrogen irradiation with the same dose ($d_H = 3 \times 10^{18}$ cm^{-2}) employed for $\text{GaAs}_{1-x}\text{N}_x$. At variance with the N-containing sample, H irradiation in GaAs causes a *decrease* of R by a factor 3, likely determined by

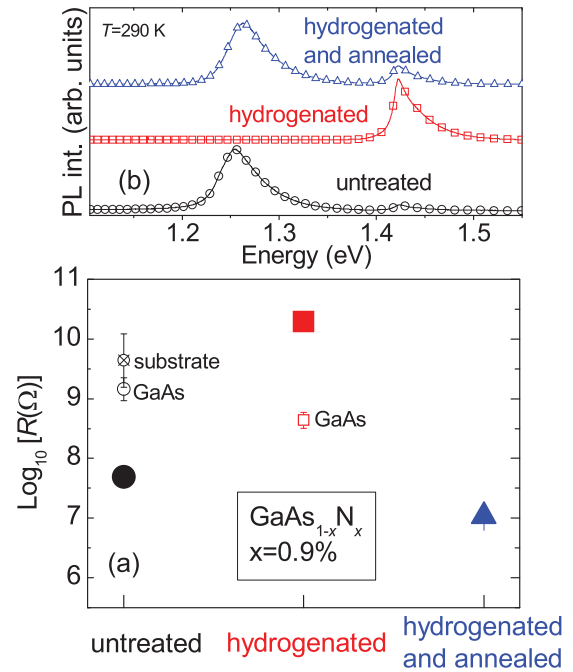


FIG. 1. (Color online) (a) Large full symbols: Values of the local resistance R in a $\text{GaAs}_{1-x}\text{N}_x$ sample (thickness 200 nm, $x = 0.9\%$ and no GaAs cap layer) subjected to different treatments as indicated in the horizontal axis. The hydrogen dose employed is $d_H = 3 \times 10^{18}$ cm^{-2} . Annealing was performed on the hydrogenated sample at temperature equal to 550°C for 1 hour. Uncertainties equal symbol size. Small open symbols: Values of R recorded on a GaAs reference sample (thickness 200 nm and grown under the same conditions of the $\text{GaAs}_{1-x}\text{N}_x$ sample) untreated and hydrogenated ($d_H = 3 \times 10^{18}$ cm^{-2}). The local resistance value of the GaAs substrate used for the samples considered in this work is also shown. (b) Room temperature PL spectra of the same samples displayed as large symbols in part (a). The peak at 1.255 eV is due to carrier recombination from the band gap of untreated $\text{GaAs}_{1-x}\text{N}_x$ and post-annealing hydrogenated $\text{GaAs}_{1-x}\text{N}_x$. The peak at 1.422 eV is due to carrier recombination from the GaAs or fully N-passivated $\text{GaAs}_{1-x}\text{N}_x$.

defect passivation.¹⁶ Moreover, R values in $\text{GaAs}_{1-x}\text{N}_x$ are sizably smaller (a factor 30) than those of the N-free control sample. This may be attributed to a larger intrinsic carrier concentration of $\text{GaAs}_{1-x}\text{N}_x$ due to its lower band-gap energy and/or to nonoptimal conditions employed to grow the GaAs reference.¹⁶ We will not dwell further on this finding, but we emphasize that R in the N-free control sample does not show major variations upon hydrogenation. We also point out that R in as-grown $\text{GaAs}_{1-x}\text{N}_x$ ($\sim 5 \times 10^7$ Ω) is smaller than in the GaAs substrate ($\sim 5 \times 10^9$ Ω) on which the $\text{GaAs}_{1-x}\text{N}_x$ layers have been deposited. This shows that the GaAs layer structure beneath $\text{GaAs}_{1-x}\text{N}_x$ does not affect sizably CP-AFM measurements in the N-containing layers.¹⁴

The dependence of R on H dose is shown in Fig. 2 for three samples with different N concentrations. Data derived by PL and/or secondary ion mass spectrometry indicate that N is fully passivated in all samples, except in the sample with $x = 1.27\%$ and $d_H = 2 \times 10^{18}$ cm^{-2} . Therein, N is fully passivated for $d_H = 5 \times 10^{18}$ cm^{-2} , and R increases by a factor of 700. In the sample with the highest N concentration ($x = 1.95\%$),

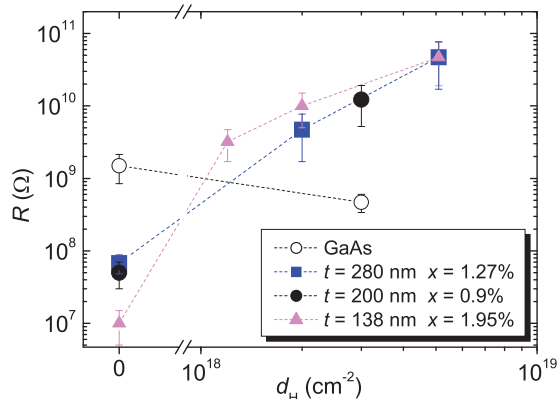


FIG. 2. (Color online) Dependence of the local resistance R on H irradiation dose, d_H , for GaAs $_{1-x}$ N $_x$ samples having different composition and thickness t .

R increases by a factor 4700 for the highest H dose. In this sample, however, full N passivation is reached already for $d_H = 1.2 \times 10^{18} \text{ cm}^{-2}$, where R increases by a factor 320. The further increase of R by a factor of ~ 15 observed ongoing from $d_H = 1.2 \times 10^{18} \text{ cm}^{-2}$ to $d_H = 5 \times 10^{18} \text{ cm}^{-2}$ could be due to H-induced defects forming in high N concentration samples.¹⁷ Nevertheless, we deem their contribution of minor importance for the other samples. In fact the hydrogenation technique we use is characterized by a low energy (100 eV) of the impinging ions that usually does not introduce damages typical of high-energy implantations.

All these results demonstrate that the electrical resistance of GaAs $_{1-x}$ N $_x$ can be sizably modulated by hydrogen irradiation in a fully controllable and reversible manner. This finding mimics the effects H has on the optical and structural properties of dilute nitrides and assigns to the N-2H complexes a rather unexpected role, that is, the capability to *modify even the transport properties of these alloys*.

Now we address the possible mechanism through which charge carrier motion is affected by these complexes. In CP-AFM measurements, the contact resistance depends on the ratio between the nanocontact size and the mean free path (MFP) of electrons flowing through the contact interface.^{14,17–20} R. Holm derived an expression for R by assuming that contact size and MFP are comparable,¹⁸ while Y. V. Sharvin derived a similar expression for contact sizes larger than the MFP.¹⁹ A term of barrier resistance is also added to take into account rectification effects at the contact surface.^{14,18,20} In the present case the Holm's expression has been used. Indeed, S. Fahy and E. P. O'Reilly²¹ found that the MFP in dilute GaAs $_{1-x}$ N $_x$ is in the 10-nm range, a value comparable or even smaller than the contact size expected between the CP-AFM tip and the sample surface. Thus, the contact resistance in our CP-AFM measurements is given by

$$R_{\text{Holm}} = \frac{\rho_{\text{sample}}}{4a}, \quad (1)$$

where ρ_{sample} designates the sample resistivity, and a is the electrical contact radius of the AFM probe. This formula also assumes that the resistivity of the AFM probe is negligible compared to the sample resistivity, that is the case here. In an intrinsic semiconductor $\rho = [en_i(\mu_e + \mu_h)]^{-1}$, where e is

the modulus of the electron charge, n_i is the intrinsic carrier concentration, and $\mu_{e,h} = (e\tau_{e,h})/m_{e,h}$ is the mobility of electrons (e) and holes (h). $m_{e,h}$ and $\tau_{e,h}$ are the carrier effective mass and mean scattering time, respectively. Since in III-V semiconductors the mobility of holes is usually much smaller than that of electrons, the resistivity can be written neglecting the hole contribution. If we make n_i explicit,²² we find

$$\rho = \frac{e^{\frac{E_g}{2k_B T}}}{\frac{e^2 \tau_e}{m_e} 2 \left(\frac{2\pi k_B T}{h^2} \right)^{\frac{3}{2}} (m_e m_h)^{\frac{3}{4}}}, \quad (2)$$

where E_g is the crystal band-gap energy at temperature T . Since the root mean square roughness of the samples is in the nanometer range ($\leq 1 \text{ nm}$) and the tip geometry of the conductive-probe microscope is always the same, we can assume that the electrical contact radius defined in Eq. (1) is comparable for all measurements. Therefore, the ratio of the resistance measured after (R_H) and before (R_N) hydrogen incorporation is given by²³

$$\frac{R_H}{R_N} = e^{\frac{E_{gH} - E_{gN}}{2k_B T}} \left(\frac{m_{eH}}{m_{eN}} \right)^{\frac{1}{4}} \frac{\tau_{eN}}{\tau_{eH}}, \quad (3)$$

where the subscripts ‘‘H’’ and ‘‘N’’ refer to H-containing and H-free GaAs $_{1-x}$ N $_x$ samples, respectively. The band-gap energy^{5,9} and the electron-effective mass^{6,7,24,25} are assumed to be known before and after H incorporation. If we set $\tau_{eN} = \tau_{eH}$ in Eq. (3), the H-induced variations of the energy gap and electron-effective mass lead to a large underestimation (a factor 10, at least) of the observed changes of R . Table I reports the room temperature band-gap energy, R_H/R_N and $\beta = \tau_{eN}/\tau_{eH}$, for each sample. In determining β , we set the electron mass equal to $0.067 m_0$ (m_0 is the electron mass in vacuum) in the fully N-passivated samples, as experimentally found.⁷ For nonhydrogenated samples we rely on magnetop-PL measurements performed on samples with similar N concentration,⁷ resulting in an electron effective mass equal to $0.12 m_0$.²⁶ All R_H/R_N and $\beta = \tau_{eN}/\tau_{eH}$ values have been calculated for the highest H dose employed; see Fig. 2. β values in Table I indicate that the carrier scattering time decreases by at least one order of magnitude as a result of the formation of nitrogen-hydrogen complexes, thus strongly suggesting that these complexes act as scattering centers. As discussed

TABLE I. Summary of the effects of H irradiation in GaAs $_{1-x}$ N $_x$ samples having different composition and thickness t . E_g is the band-gap energy at room temperature of the as-grown samples (after H irradiation the band-gap energy is equal to that of GaAs, 1.422 eV, for all samples), R_H/R_N is the ratio of the local resistance values measured after, R_H , and before, R_N , hydrogen incorporation. $\beta = \tau_{eN}/\tau_{eH}$ quantifies the reduction of electron scattering time upon hydrogenation (τ_{eN} and τ_{eH} refer to the sample before and after H incorporation, respectively).

sample	E_g (eV)	R_H/R_N	$\beta = \tau_{eN}/\tau_{eH}$
$x = 0.90\%$, $t = 200 \text{ nm}$	1.250	470	18
$x = 1.27\%$, $t = 280 \text{ nm}$	1.200	690	10
$x = 1.95\%$, $t = 138 \text{ nm}$	1.112	4700	12

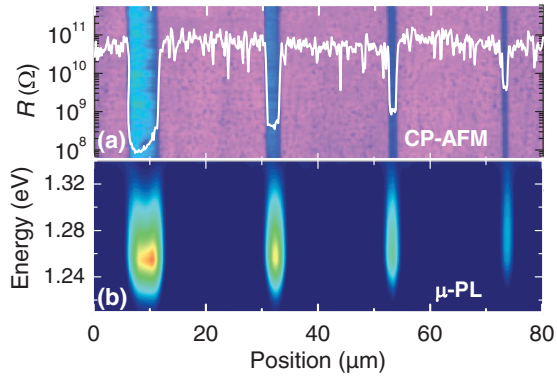


FIG. 3. (Color online) (a) CP-AFM two-dimensional mapping of the local resistance R of a $\text{GaAs}_{1-x}\text{N}_x$ sample ($x = 0.9\%$ and $t = 200$ nm), whose surface was patterned before H irradiation by H-opaque titanium wires having width equal to 5, 2, 1, and $0.5 \mu\text{m}$ (from left to right), each separated by $20 \mu\text{m}$. The white line superimposed on the two-dimensional mapping of R provides the value of the local electrical resistance (ordinate axis) along a line perpendicular to the axis of the wires. (b) One-dimensional mapping of the μ -PL intensity across the wire region recorded at room temperature. The abscissa axis indicates the laser spot position. The ordinate axis indicates the energy of the emitted photons. The emission intensity is shown in a false color scale (red and blue corresponds to maximum and minimum intensity, respectively). Maximum intensity in the region between wires is found at 1.422 eV, namely the GaAs band gap energy (not shown here).

previously, some contribution to the R increase from different centers may be possible for $x \sim 2\%$.

Finally we present an interesting outcome of our findings, that is, the possibility to pattern the electrical properties of $\text{GaAs}_{1-x}\text{N}_x$ in its growth plane with submicrometer spatial resolution. Figure 3(a) shows a CP-AFM two-dimensional mapping of the local electrical resistance of a series of $\text{GaAs}_{1-x}\text{N}_x$ wires separated by GaAs-like barriers. The wires having different width w were formed by spatially selective hydrogenation^{2,9} of the $t = 200$ nm and $x = 0.9\%$ sample, as detailed in the Experimental section.²⁷ Resistance imaging shows that R is much lower in the H-free regions than between the wires, where $R \sim 6 \times 10^{10} \Omega$. This is well evidenced by the linear scan of R perpendicularly to the wire axis and superimposed to the CP-AFM image in Fig. 3(a). The ratio of the local resistance between the N-passivated barriers

and the $\text{GaAs}_{1-x}\text{N}_x$ wires varies from a factor 750 to 15 on going from $w = 5 \mu\text{m}$ to $w = 0.5 \mu\text{m}$. This dependence on w is due to H lateral diffusion beneath the metallic wires that tends to increase the effective local resistance of the considered wire, this effect being more pronounced for smaller w . Indeed, secondary ion-mass spectrometry performed on the same sample shows a deuterium decay length equal to 12 nm/decade for hydrogenation temperature of 300°C .¹⁰ Combined with current spreading from the probe nanocontact, this leads to an effective local resistance profile that reduces by a factor 10 within 150 nm at most at the border between hydrogenated and nonhydrogenated regions. This in-plane electrical modulation mirrors the spatial variation of the band-gap energy as determined by μ -PL measurements shown in Fig. 3(b) for the same artificial structure displayed in Fig. 3(a). The wire region emits at the band-gap energy of the as-grown sample (about 1.25 eV), whereas the regions aside the wire emit at higher energy (1.422 eV, namely the GaAs band gap). The lower resistance regions of the planar heterostructure clearly coincide with those having the smaller band-gap energy.

IV. CONCLUSIONS

In conclusion we reported a peculiar effect concerning the electrical properties of $\text{GaAs}_{1-x}\text{N}_x$ following hydrogen incorporation. A giant enhancement in the local resistance is observed concomitantly with the neutralization of the electronic activity of nitrogen in $\text{GaAs}_{1-x}\text{N}_x$. This phenomenon is ascribed to two processes. The first is a decrease in the intrinsic carrier concentration due to the band gap increase upon hydrogenation. The second is a tenfold, or more, reduction of the carrier scattering time most likely due to the nitrogen-hydrogen complexes responsible for N passivation. Finally, $\text{GaAs}_{1-x}\text{N}_x$ fully recovers its electrical properties after the nitrogen-hydrogen complexes are removed by thermal annealing. These effects can be exploited for the realization of microscopic circuits, such as on-chip microscale coils, and of electrical interconnects of more complicated nanostructures fabricated by the masked-hydrogenation procedure outlined in this work.

ACKNOWLEDGMENTS

This work was supported by the COST Action MP0805.

*Corresponding author: antonio.polimeni@roma1.infn.it

¹For a review see: *Physics and Applications of Dilute Nitrides*, edited by I. A. Buyanova and W. M. Chen (Taylor & Francis Books Inc., New York, 2004); *Dilute Nitride Semiconductors*, edited by M. Henini (Elsevier, Oxford UK, 2005); *Dilute III-V Nitride Semiconductors and Material Systems*, edited by Ayse Erol (Springer, Berlin, Germany, 2008).

²M. Felici, A. Polimeni, G. Salviati, L. Lazzarini, N. Armani, F. Masia, M. Capizzi, F. Martelli, M. Lazzarino, G. Bais, M. Piccin, S. Rubini, A. Franciosi, *Adv. Mater.* **18**, 1993 (2006).

³L. Wen, F. Bekisli, M. Stavola, W. B. Fowler, R. Trotta, A. Polimeni, M. Capizzi, S. Rubini, and F. Martelli, *Phys. Rev. B* **81**, 233201 (2010).

⁴Marina Berti, Gabriele Bisognin, Davide De Salvador, Enrico Napolitani, Silvia Vangelista, Antonio Polimeni, Mario Capizzi, Federico Boscherini, Gianluca Ciatto, Silvia Rubini, Faustino Martelli, and Alfonso Franciosi, *Phys. Rev. B* **76**, 205323 (2007).

⁵G. Baldassarri, H. v. H., M. Bissiri, A. Polimeni, M. Capizzi, M. Fischer, M. Reinhardt, and A. Forchel, *Appl. Phys. Lett.* **78**, 3472 (2001).

- ⁶E. P. O'Reilly, A. Lindsay, P. J. Klar, A. Polimeni, and M. Capizzi, *Semicond. Sci. Technol.* **24**, 033001 (2009).
- ⁷F. Masia, G. Pettinari, A. Polimeni, M. Felici, A. Miriametro, M. Capizzi, A. Lindsay, S. B. Healy, E. P. O'Reilly, A. Cristofoli, G. Bais, M. Piccin, S. Rubini, F. Martelli, A. Franciosi, P. J. Klar, K. Volz, and W. Stolz, *Phys. Rev. B* **73**, 073201 (2006).
- ⁸M. Geddo, M. Patrini, G. Guizzetti, M. Galli, R. Trotta, A. Polimeni, M. Capizzi, F. Martelli, and S. Rubini, *J. Appl. Phys.* **109**, 123511 (2011).
- ⁹R. Trotta, A. Polimeni, M. Capizzi, F. Martelli, S. Rubini, M. Francardi, A. Gerardino, and L. Mariucci, *Appl. Phys. Lett.* **94**, 261905 (2009).
- ¹⁰R. Trotta, D. Giubertoni, A. Polimeni, M. Bersani, M. Capizzi, F. Martelli, S. Rubini, G. Bisognin, and M. Berti, *Phys. Rev. B* **80**, 195206 (2009).
- ¹¹Rinaldo Trotta, Antonio Polimeni, Faustino Martelli, Giorgio Pettinari, Mario Capizzi, Laura Felisari, Silvia Rubini, Marco Francardi, Annamaria Gerardino, Peter C. M. Christianen, and Jan C. Maan, *Adv. Mat.* **23**, 2706 (2011).
- ¹²Ryan O'Hayre, Minhwan Lee, and Fritz B. Prinz, *J. Appl. Phys.* **95**, 8382 (2004).
- ¹³J. Alvarez, F. Houze', J. P. Kleider, M. Y. Liao, and Y. Koide, *Superlattices and Microst.* **40**, 343 (2006).
- ¹⁴P. Eyben, W. Vandervorst, D. Alvarez, M. Xu, and M. Fouchier, *Scanning Probe Microscopy*, edited by S. Kalinin and A. Gruverman (Springer, New York, 2007), vol. I, Chap. 1, p. 31.
- ¹⁵We verified that the thermal treatment used during H irradiation (3 hours at 300 °C) does not cause sizable variations of R .
- ¹⁶For comparison purposes, the reference N-free sample was grown with the same growth protocol of GaAs_{1-x}N_x, which could not be not suitable for GaAs.
- ¹⁷A. Polimeni, G. Baldassarri H. v. H., M. Bissiri, M. Capizzi, M. Fischer, M. Reinhardt, and A. Forchel, *Phys. Rev. B* **63**, 201304(R) (2001).
- ¹⁸R. Holm, *Electric Contacts Theory and Applications*, (Springer, Berlin, 2000), pp. 9–52.
- ¹⁹Y. V. Sharvin, *Soviet Physics JEPT* **21**, 655 (1965).
- ²⁰L. Weber, M. Lehr, and E. Gmalin, *Phys. Rev. B* **43**, 4317 (1991).
- ²¹S. Fahy and E. P. O'Reilly, *Appl. Phys. Lett.* **83**, 3731 (2003).
- ²²Ben G. Streetman, *Solid State Electronic Devices*, (Prentice-Hall International Editions, Englewood Cliffs, NJ, 1990), p. 78.
- ²³The hole effective mass does not change with N and hence with H.
- ²⁴T. Dannecker, Y. Jin, H. Cheng, C. F. Gorman, J. Buckeridge, C. Uher, S. Fahy, C. Kurdak, and R. S. Goldman, *Phys. Rev. B* **82**, 125203 (2010).
- ²⁵G. Allison, S. Spasov, A. Patanè, L. Eaves, N. V. Kozlova, J. Freudenberger, M. Hopkinson, and G. Hill, *Phys. Rev. B* **77**, 125210 (2008).
- ²⁶The factor β reported in Table 1 varies by 8% at most for an electron mass varying between 0.12 m_0 and 0.16 m_0 (namely, the range of variation of the electron mass shown in Fig. 3 of Ref. 7 for the N concentrations of the samples investigated here).
- ²⁷We point out that no Ti residuals were present after removal of the metallic wires, as indicated by topographic AFM images of the sample surface acquired concomitantly with the local resistance mapping.